Learning from native defects on EUV mask blanks

Emily Gallagher[a], Alfred Wagner[b], Mark Lawliss[a], Gregory McIntyre[c], Kazunori Seki[d], Takeshi Isogawa[d], Steven Nash[a]

[a]IBM Microelectronics Div., 1000 River Street, Essex Junction, VT 05452
[b]IBM Research Div., 1101 Kitchawan Rd, Yorktown Heights, NY 10598
[c]IBM Microelectronics Div., 257 Fuller Road, Albany, NY 12203
[d]Toppan Photomasks Inc., 1000 River Street, Essex Junction, VT 05452

ABSTRACT

Defects in the EUV mask blank are one of the largest hurdles to achieving manufacturing readiness of EUV masks. For defect-free masks, the obvious approach is to order blanks that do not have defects or to shift the pattern so that remaining defects do not create a printed defect on wafer. The approach during development should be different. At this learning phase, it is wise to study the defects as they occur naturally on the EUV mask blank. This paper outlines a comprehensive approach to building a mask specifically to showcase the native defects so that they can be studied and repairs can be attempted. The method applied to mask build, defect inspection and characterization will be reviewed in detail. Printability of the mask defects of interest are characterized using both wafer printing and EUV microscope data. Repairs are attempted and characterized. In the end, the impact of native defects is discussed along with the viability of various repair methods.

Keywords: EUV, mask defect repair, defect printability

1 INTRODUCTION

A defect free patterning solution relies on a mask free of printable defects. At this point in EUV development, the mask blanks used to build the EUV masks are not defect free.[1] Consequently the industry is attacking the mask defect problem on multiple fronts. The most obvious solution is eliminating defects in the mask blank. While progress has been made, most assume that there must be a parallel effort to address EUV mask blank defects during and after mask build. During mask build, multilayer defect size and location can be fed forward from the multilayer inspection to the mask pattern write step. The pattern can be shifted within centrality limits of lithography to ensure that clear patterns avoid the multilayer defect region [2]. This is shown in Figure 1.

While pattern shifting to avoid defects has been demonstrated in principle, there are still many aspects of the pattern shift that require development. Identifying the defects' coordinates with sufficient accuracy is one challenge. For now, a margin for error is included in location calculations. This margin will shrink over time with improved blank inspection stages and fiducial marking practices. A second challenge is determining the lithographic impact of blank defects. Inspections are not currently actinic, but are typically performed at 193nm or some other optical wavelength. The impact of the defect is important for several reasons. The most obvious is that the defect's EUV impact defines the absorber region size needed to cover the multilayer defect. A related reason for quantifying the impact of a defect is to perform triage on the blank defect

Photomask and Next-Generation Lithography Mask Technology XXI, edited
by Kokoro Kato, Proc. of SPIE Vol. 9256, 92560K · © 2014 SPIE
CCC code: 0277-786X/14/$18 · doi: 10.1117/12.2070871

Downloaded From: http://proceedings.spiedigitallibrary.org/ on 11/25/2014 Terms of Use: http://spiedl.org/terms

sample – determining which defects are likely to result in a printable defect on the final mask, which should be covered with absorber through pattern shift, and which might be repaired by conventional mask repair methods. Sematech recently reported a lack of correlation between defect size and printability.[3] In this paper, we expand defect characterization beyond the physical view of the defect on the mask that can be obtained from scanning electron microscope (SEM) and atomic force microscope (AFM) to explore other possible mask indicators for printing impact. In Section 2, we describe our method for determining the printability of the mask defects after they have been characterized on the mask blank.In Section 3, we combine the blank inspection with mask characterization data and defect printability to establish correlations between printability and the initial blank defect. The ultimate goal the goal is to identify wafer printability as early as possible in the mask build. Section 4 is a sample case of two defect repairs. Finally the results are placed in perspective, with suggestions for the future EUV mask blank requirements.

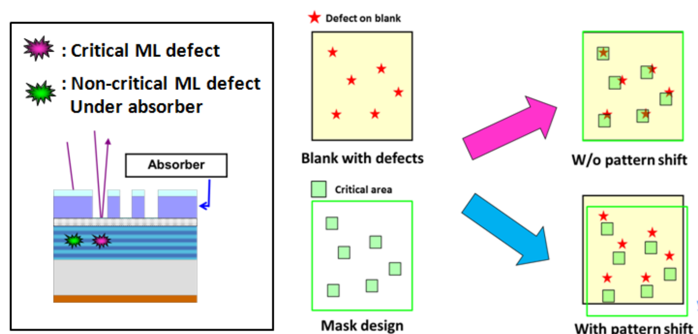

Figure 1. A schematic view of pattern shift for defect avoidance is illustrated. The boxed image on the left shows the final mask in cross-section with two multilayer defects. The defect located under the absorber is non-critical, while the one in the clear region is critical. To the right a flow diagram of a blank with defects and a mask design are merged with and without pattern shift. The lower pattern with the pattern shift illustrates the effectiveness of a shift to place all defects away from clear regions.

2 MASK BUILDS AND DATA COLLECTION

2.1 Blank inspection background

The two EUV mask blanks used in this work had standard films: 2.5nm of Ru-capping layer, 40 pairs of Mo/Si bi-layers on the substrate and CrN on the back side. 193nm blank inspections were performed and a set of defects identified for each mask blank. Care was taken to record and analyze the inspection output. There are two obvious metrics that can be extracted: size and residual. Inspection defect sizes are given in x and y directions and are obtained from the extent of the grayscale difference image and automatically reported. The residual is different; it is the maximum grayscale residual of a group of pixels associated with a defective region. Both inspection metrics are shown in Figure 2. It is important to note that defect size does not correlate to residual, but either size or residual could correlate to printing impact.

Figure 2. A defect image obtained at 193nm is shown on the left, with size in x and y superimposed. The smaller defect images on the right illustrate that size and residual do not always correlate: the defect that is larger has a smaller residual signal in this case.

Downloaded From: http://proceedings.spiedigitallibrary.org/ on 11/25/2014 Terms of Use: http://spiedl.org/terms

2.2 Method for creating a native defect test mask

The introduction described pattern shift as a method that can be used to avoid defects. Since our goal is to study defects and their printability, we applied the reverse of defect avoidance, shifting the patterns to place clear areas over identified blank defects as is illustrated in Figure 2. A method for creating a native defect test mask includes: adding fiducial marks to the blank, inspecting the blank aligned to the reference fiducial to obtain defect coordinates, creating a mask pattern to place patterns centered on the native defects. Standard Ta-based EUV mask absorber was deposited and chemically amplified electron beam resist applied. Two pattern files were created placing known patterns at the known location of the defects of interest. For Mask 1, the pattern was a 5 x 5 contact hole array, 160nm contacts on a 1:1 pitch. For Mask 2, the pattern was 160nm lines and spaces, again on a 1:1 pitch. Our objective is to create a pattern for defect location, but not to challenge lithography or tie the results to a specific node. The pattern files that were created are specifically linked to the a priori knowledge of a single blank's defect locations and could not be used effectively on a different blank.

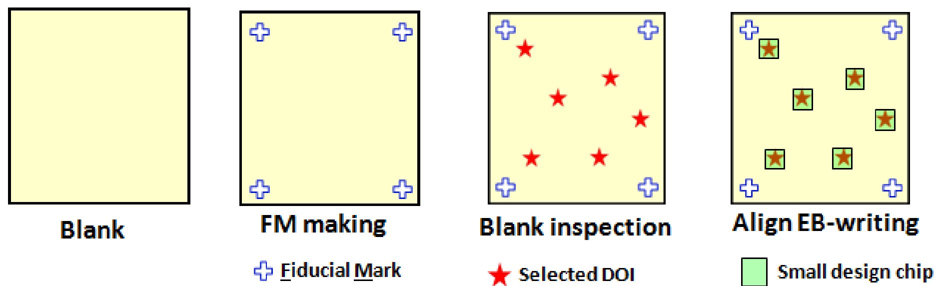

Figure 3. A method for creating a native defect test mask includes: adding fiducial marks to the blank, inspecting the blank aligned to the reference fiducial to obtain defect coordinates, creating a mask pattern to place features centered on the native defects.

The two masks were written using standard 50keV electron beam write tools, develop, etch and strip processes. The effectiveness of the overlay is shown in Figure 4. The intent was to center all defects on the center contact, and the results are good but not perfect: all defects are less than 100nm from the center of the target contact. Similar results were found on Mask 1, but only the contact mask is shown because it is inherently better for illustrating results in two dimensions. It is worth noting that the range of defect locations, while initially unintentional, created realistic printability and repair sites.

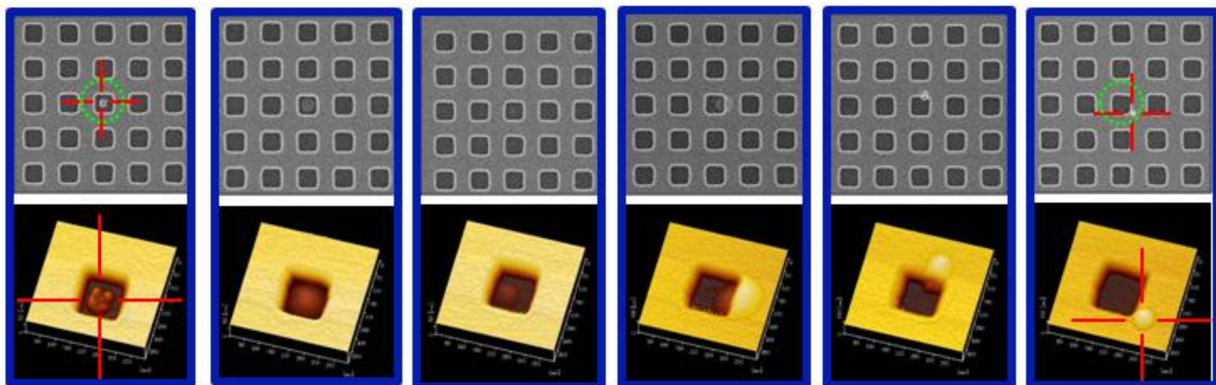

Figure 4. CDSEM images from Mask1 are shown on the top row with the corresponding AFM scans below. Cross-hairs are shown on the far right and left images to guide the eye. In the left image, the defect is closest to center. The image pair progression shows a range of outcomes with the worst at the far right. The intent was to center all defects on the center contact. All defects are less than 100nm from the center of the target contact and some are large enough to impact multiple contacts.

Downloaded From: http://proceedings.spiedigitallibrary.org/ on 11/25/2014 Terms of Use: http://spiedl.org/terms

The mask defects were then assessed for printability in two ways: using an EUV microscope [4] and imaging on wafer. Consistent with the design selection, determining basic printability is the goal. Details of wafer resist and illumination conditions were not explored. Wafer images like the ones shown in Figure 5 are used to determine printability. If the contact is missing or shows a dramatic CD change, the defect is printable. If the center contact appears slightly different from the others, the defect printability is marginal. If there is no clear difference between the target contact and the surrounding ones, the defect it not printable. Wafer results include resist effects, so we confirmed the printability classifications with the EUV microscope. Armed with this classification, we attempt to determine a link between printability and mask inspection in Section 3.

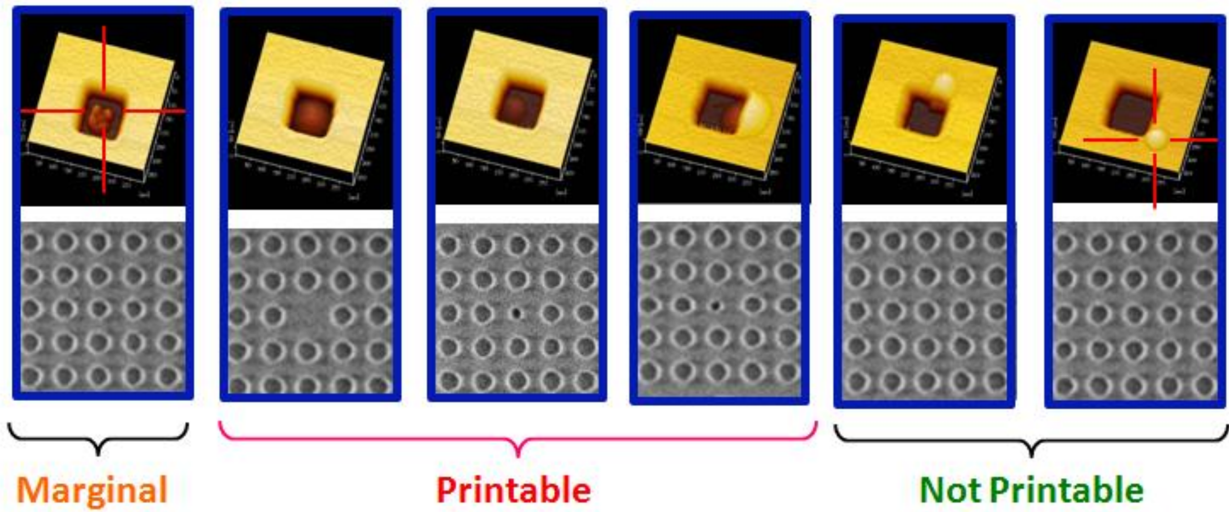

Figure 5. The six defects from Figure 4 are shown again, in the same order. The AFM image is shown on the top row with the associated wafer image below. Based on the wafer result, three categories of printability are determined: marginal, printable and not printable.

3 RESULTS AND DISCUSSIONS

3.1 Printability with Mask 1, contact patterns

A visual plot was created by combining the multilayer blank inspection results and the printability assessment. Defect area is obtained by simply multiplying the x and y sizes. More subtle calculations could be performed, but did not change the results in a meaningful way. Remaining close to the defect reports makes future use of the data simpler. Figure 6 shows a plot of defect residual vs. defect area for the contact pattern. The printability dimension is introduced by using three plotting shapes: the circle for printable, the triangle for marginal and the diamond for not printable defects. There are two distinct regions. Inside the gray box, the defects sometimes print, but do not always. Outside the gray box, where the multilayer defect was either large or had a large residual, the defects always print. Looking more carefully within the gray zone defined by a residual of 300 and an area of $1*10^6$ nm^2, there is no obvious link between the AFM images and the defect printability. We looked at defect location relative to the contact center, defect size and defect shape and none showed a systematic correlation to printability.

Downloaded From: http://proceedings.spiedigitallibrary.org/ on 11/25/2014 Terms of Use: http://spiedl.org/terms

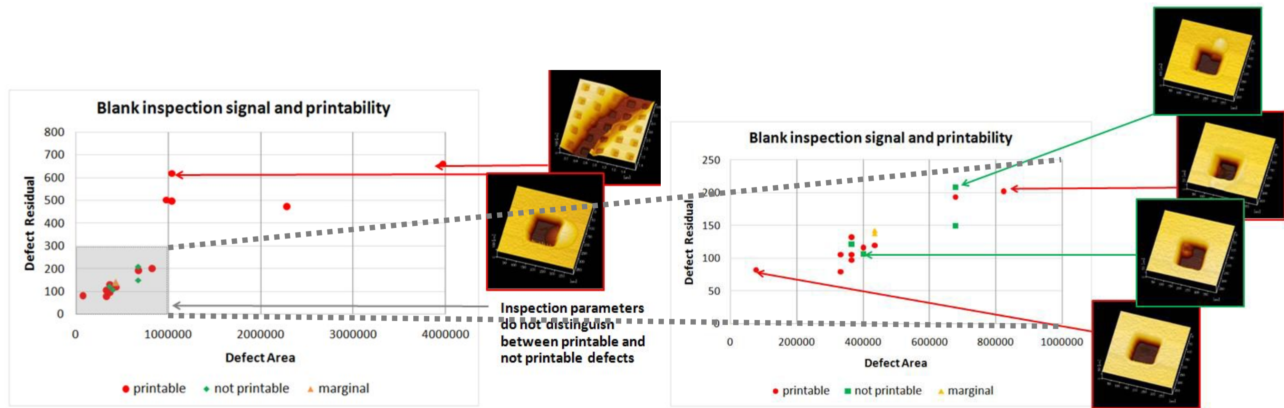

Figure 6. Two plots of defect residual vs. defect area for the contact pattern are shown. The printability dimension is added by introducing three plotting shapes: the circle for printable, the triangle for marginal and the diamond for not printable defects. The left plot shows the full range of data. The right one is a magnified view of the gray box where printable, marginal and non-printable defects coexist.

3.2 Printability with Mask 2, line and space patterns

Figure 7 shows a plot of defect residual vs. defect area for the line space pattern. The printability dimension is again introduced by using three plotting shapes: the circle for printable, the triangle for marginal and the diamond for not printable defects. With one exception, the same conclusion can be reached. Examining the SEM of the exceptional defect, it is clear that the defect does note intersect any clear area. Again, the general result is that inside the gray zone defined by a residual of 300 and an area of $1*10^6$ nm^2, printable, marginally printable and not printable defects coexist.

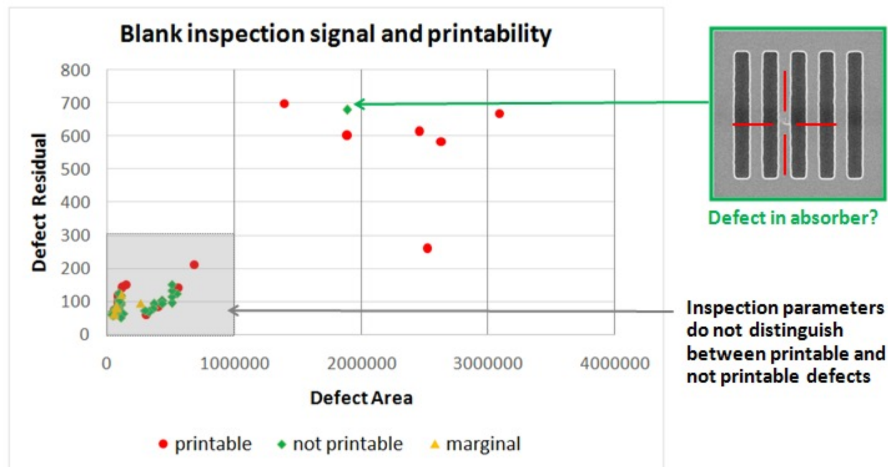

Figure 7. A plot of defect residual vs. defect area for the line space pattern is shown. The printability dimension is added by introducing three plotting shapes: the circle for printable, the triangle for marginal and the diamond for not printable defects. The gray box indicates the region where printable, marginal and non-printable defects coexist.

4 REPAIR

Any complete mask process includes repair. This work is linked to the initial work in several ways. The first is that the same masks are used. More significantly we attempted to use the signature of the defects at blank inspection to group like defects so that we could apply similar repair methods to mitigate their impact. We selected two multilayer defects for repair testing, shown in Figure 8.

Downloaded From: http://proceedings.spiedigitallibrary.org/ on 11/25/2014 Terms of Use: http://spiedl.org/terms

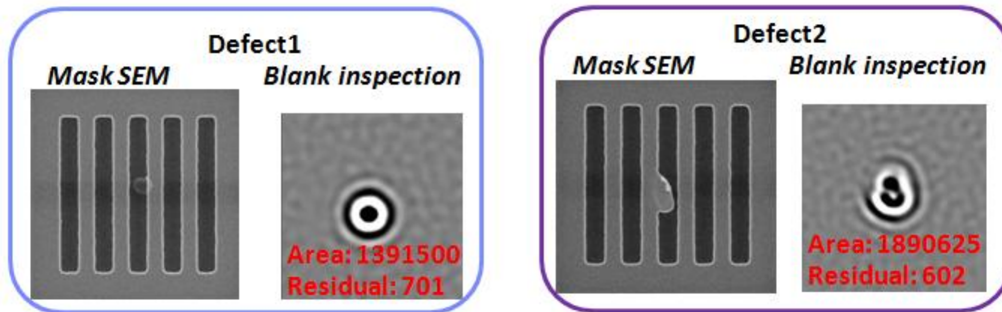

Figure 8. CDSEM and 193nm blank inspection images of the defects selected for repair. Blank multilayer inspection images at 193nm are shown with the associated area and residual. Both defects appear quite similar. The CDSEM image differs, but indicates very similar alignment relative to the center line.

These defects were both detected during blank inspection, and therefore not created during mask processing. The pattern printed over the defects was a 160nm line/space pattern, with the target location of the defect being the center space of the array. In both cases, the defect was successfully placed in the center space and transitioned into an adjacent line. This pattern size and design was chosen for straightforward printability analysis and repair. Pre-repair metrology was obtained with both wafer prints through focus and on an EUV microscope with two illumination NA's, 0.25 and 0.33. Both the wafer print and the EUV microscope images shown in Figure 9 indicate a catastrophic print error with the space completely bridged for both defects.

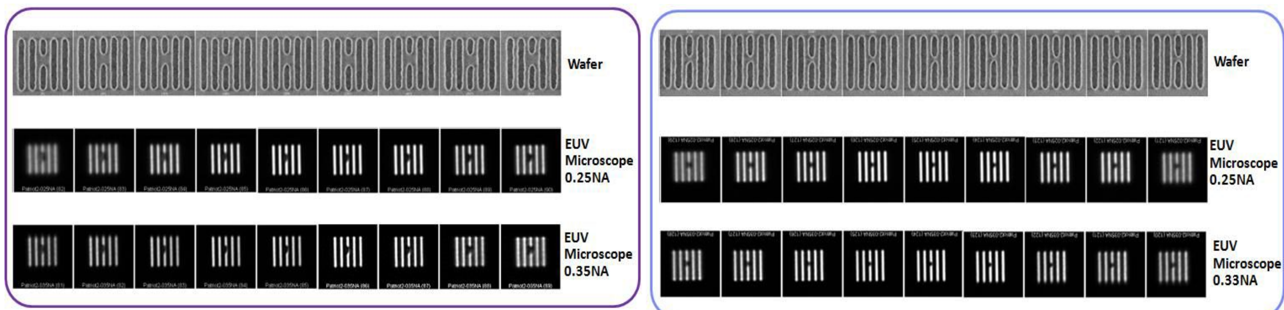

Figure 9. Pre-repair characterization of Defect 1 (left) and Defect 2 (right) indicate a complete bridge on the central line and very similar through focus response. Each row is a collection of images through focus with best focus in the center. The top row is the wafer result, the middle row is the 0.25NA microscope images and the bottom row is 0.33NA microscope images.

The repair testing was completed using a nanomachining system. Our approach was to remove the defect in the clear space down to the capping layer and to add a small absorber bias (<10nm) on the line edge adjacent to the defect. The repair debris created was then removed with the standard post-repair clean. As shown in the post repair SEM's and AFM's of Figure 10, the defect repair was executed exactly as planned in both cases. These post-repair measurements predict equally good printability on both sites.

Downloaded From: http://proceedings.spiedigitallibrary.org/ on 11/25/2014 Terms of Use: http://spiedl.org/terms

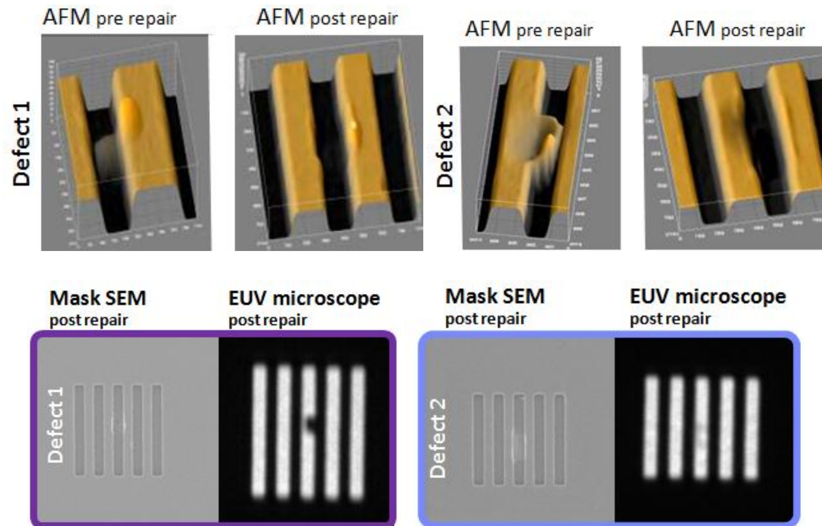

Figure 10. Defect 1 is shown in the four images on the left and Defect 2 images are on the right. For each defect the pre and post repair AFMs are shown on top indicating a perfectly executed repair. The lower images show the SEM post repair and finally the EUV microscope assessment of printability.

Post repair metrology on the same EUV microscope with the same illumination NA's used pre-repair provided a surprising result. The same repair approach was used for both defects. Defect 1 showed only marginal print improvement and was still a catastrophic bridging defect. Conversely, Defect 2 printed well with <10% CD error. In both cases, re-repair options could be considered to improve printability. To make a small improvement to Defect 2, an increased absorber bias would be attempted. For Defect 1, a more significant re-repair would be considered, including more aggressive absorber bias on both edges and possibly ML repair. Edits to Defect 1 are less likely to improve the result. This example highlights the challenge of repairing multilayer defects. Success is possible, but not at all certain. Pure absorber defects are not the concern since they can be addressed with repair options that are standard in the industry. We are specifically highlighting the difficulty of achieving a predictable outcome when attempting to repair multilayer defects.

5 SUMMARY

A method for studying native multilayer defects was described. Patterns were placed directly over multilayer defects so that their printability could be assessed. A complete set of data on defects was collected: blank defect inspection signal at 193nm, mask SEM, mask AFM, EUV microscope images and wafer print images. While we had hoped to identify something that could be measured on the mask to predict printability, we instead were able to define three zones based on the blank multilayer inspection metrics of defect residual and defect area. These zones are illustrated in Figure 11. For the smallest defects, characterized by residuals that are smaller than~ 300 and the defect area that is smaller than $\sim 1*10^6$ nm^2, a repair method must be developed. The largest blank defects, with defect residual larger than ~ 500 and area larger than $\sim 3*10^6$ nm^2, must be eliminated from the process. For those defects in the middle zone, defect avoidance methods must be deployed to mitigate their impact by placing them either under the absorber or in regions where defects are not a concern. Future work will focus on developing a more complete understanding of the smallest defects that should be repaired.

Downloaded From: http://proceedings.spiedigitallibrary.org/ on 11/25/2014 Terms of Use: http://spiedl.org/terms

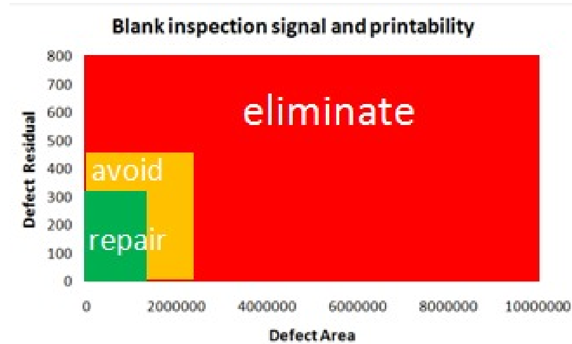

Figure 11. Defect categories as defined in the above graph by their defect residual and defect area as obtained from the multilayer blank inspection at 193nm. There are three zones shown schematically. The smallest defects should be repaired, the largest should be eliminated and the zone between should be avoided using pattern shifting techniques.

ACKNOWLEDGEMENTS

The authors would like to thank the following groups for their contributions to this paper: the RAVE LLC for EUV repairs and imaging, the SEMATECH/LBNL SHARP* team for microscope images, IBM manufacturing teams in Burlington and Albany for mask processing. Finally we would like to thank the IBM and Toppan management and technical teams for support of this project.

*SHARP work was performed under the auspices of the U.S. Department of Energy by the University of California Lawrence Berkeley National Laboratory under management and operating contract DE-AC02-05CH11231.

REFERENCES

[1] Antohe, Alin O., et al. "Production of EUV mask blanks with low killer defects." Proc. SPIE 9048, Extreme Ultraviolet (EUV) Lithography V, 90480H (2014).

[2] Negishi, Y., et al, “Using pattern shift to avoid blank defects during EUVL mask fabrication” Proc. SPIE 8701, 870112 (2013).

[3] Kwon, H.K., et al, “Printability of native blank defects and programmed defects and their stack structures” Proc. SPIE 8166, 81660H (2011).

[4] Kenneth A. Goldberg et al., “The SEMATECH high-NA actinic reticle review project (SHARP) EUV mask-imaging microscope” Proc. SPIE 8880, 88800T-1 (2013).

Downloaded From: http://proceedings.spiedigitallibrary.org/ on 11/25/2014 Terms of Use: http://spiedl.org/terms